

Adaptive mesh generation by bubble packing method

Jeong-Hun Kim[†], Hyun-Gyu Kim[‡], Byung-Chai Lee^{‡†} and Seyoung Im^{‡†}

Department of Mechanical Engineering (ME3028), Korea Advanced Institute of Science and Technology,
Science Town, DaeJeon 305-701, South Korea

(Received May 13, 2002, Accepted December 6, 2002)

Abstract. The bubble packing method is implemented for adaptive mesh generation in two and three dimensions. Bubbles on the boundary of a three-dimensional domain are controlled independently of the interior bubbles in the domain, and a modified octree technique is employed to place initial bubbles in the three-dimensional zone. Numerical comparisons are made with other mesh generation techniques to demonstrate the effectiveness of the present bubble packing scheme for two- and three-dimensional domains. It is shown that this bubble packing method provides a high quality of mesh and affordable control of mesh density as well.

Key words: mesh generation; bubble packing method; modified octree; error estimator; mesh density function.

1. Introduction

Many researchers have endeavored to improve the performance of the finite element method. Among others, mesh generation is an important topic in many engineering fields. Particularly, the mesh generation of three-dimensional bodies requires a tedious work as well as a significant amount of time. Therefore, adaptive mesh generation techniques accompanied with the development of FEM have been improved to reduce efforts for constructing meshes.

One of the promising techniques is the Delaunay triangulation, which has attracted attention to many researchers for the past several decades. Rivara (1997) suggested a method of mesh generation based on the centers of the longest edges, and Boender (1994) presented a technique for an improvement of the quality of mesh by placing additional nodes on the lines crossing the centers of gravity. Many methods (Borouchaki and George 1996, Borouchaki and Lo 1995, Weatherill 1994) have been proposed to generate a mesh in three-dimensional domains. The advancing front methods (Lohner 1996) were proposed to construct a mesh by advancing a set of nodes, which have been applied to commercial programs owing to a high quality of mesh. Lo (1989) proposed a method for a convex boundary, and Frey *et al.* (1998) suggested a method for improving the mesh quality by imposing the Delaunay triangulation on the advancing front methods.

Shimada *et al.* (1997) and Yamakawa and Shimada (2000) proposed the bubble packing methods

[†] Graduate Student

[‡] Post-doctoral Fellow

^{‡†} Professor

based on a physical model. The bubble packing methods determine nodal positions, and the Delaunay triangulation technique is used to generate a mesh. Cingoski *et al.* (1997) proposed a new bubble packing technique for two-dimensional domains, in which the sizes of the bubbles are determined efficiently, and Yokoyama *et al.* (1999) suggested an algorithm for three-dimensional bubble packing. The bubble packing methods use the Miller's method (1998) to insert bubbles in a domain. The domain is ultimately filled with bubbles wherein van der Waals forces generated between the neighboring bubbles are in equilibrium. In general, the bubble packing methods give rise to a high quality of mesh because ill-shaped elements are automatically modified by a relaxation procedure. A proper error estimator is needed to determine a mesh density, which is in general required to take the larger value in the zone of the higher stress gradient. One of popular methods for error estimation is the Zienkiewicz and Zhu (Z^2) error estimator (Zienkiewicz and Zhu 1989, 1991), which shows an excellent performance in linear elastic problems. Samuelsson *et al.* (1993) and Dwyer and Evans (1997) presented improved methods for automatic mesh generation. Recently, Lee *et al.* (2000) and Choi *et al.* (2002) employed the bubble packing method for an adaptive analysis in the element free Galerkin method.

In this paper, we proposed an efficient method for a mesh generation by combining the Z^2 error estimator and the bubble packing method in two and three dimensions. The bubbles on three-dimensional boundary surfaces are controlled independently to obtain an improved quality of mesh in three dimensions. The modified octree technique (Yerry and Shephard 1984) is employed to place initial bubbles in three-dimensional bodies. Numerical examples show good performances of the present method for automatic mesh generation.

2. Bubble packing method

The Delaunay triangulation (George 1991, Bowyer 1981, Watson 1981) for an automatic mesh generation has been successfully applied to two- and three-dimensional geometries. To obtain a good quality of mesh, positions of nodes for mesh generation should be determined properly and economically. Recently, the bubble packing method, based upon the physical concept of packing bubbles inside a given domain, has been introduced as a promising technique. In this method, bubbles move in a domain until forces between bubbles are stabilized, and the Delaunay triangulation is then applied to generate a mesh connecting the nodes defined by the bubble packing method. Fig. 1 illustrates the Delaunay triangulation and the bubble packing method, and Fig. 2 shows the procedure of the bubble packing method. In this procedure, the mesh density is needed to

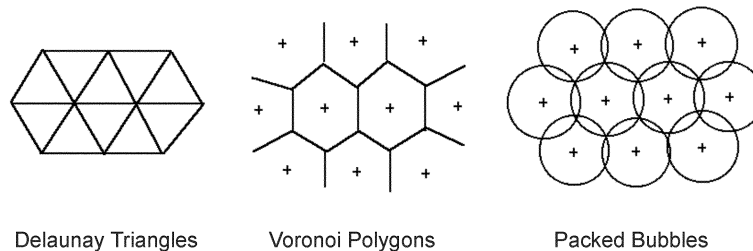


Fig. 1 Schematics of the Delaunay triangulation, the Voronoi diagram and the bubble packing method

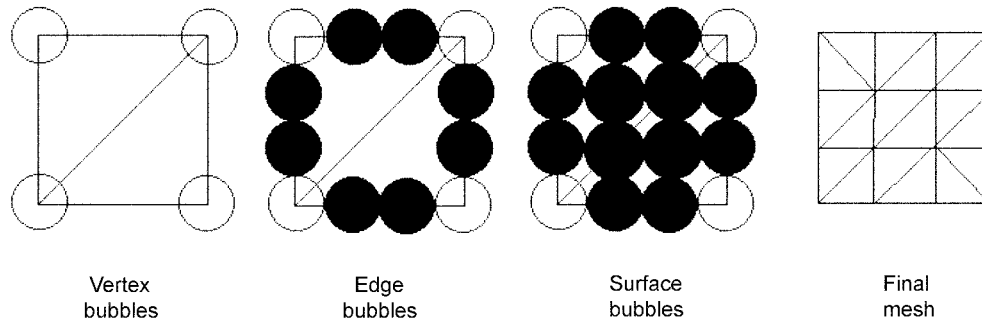


Fig. 2 Algorithm of the bubble packing method

determine the radii of bubbles. Cingoski *et al.* (1997) proposed a method to calculate the radii of bubbles to preserve some requirements.

2.1 Initial positions of the bubbles

Initial positions of the bubbles are important in the bubble packing method because the iteration procedure to reach the optimal mesh is affected by the initial conditions. In other words, a good initial guess may greatly reduce the calculation time of the relaxation described in the next section.

The initial bubbles in two dimensions are determined as follows:

1. Bubbles at the corners are created. Cingoski *et al.* (1997) calculated the radii of the bubbles by taking proportional sizes of the values at the boundaries. They inserted bubbles from the largest one on the basis of the mesh density functions. However, in this study, we add the bubbles from the smallest one. The present method provides a convenience in the control of the number of bubbles on the edges to obtain a high quality of mesh.
2. Bubbles are inserted on the edges. Positions of bubbles on the edges are adjusted based on the one-dimensional calculation because the bubbles on the edges can move along the edge lines.
3. Bubbles are created on the surfaces. We used the method proposed by Cingoski *et al.* (1997), in which nodes are distributed on regular triangles or rectangles mapped from the partitioned regions.

On the contrary to the simple procedure in the two-dimensional domains, initial bubbles in the three-dimensional bodies are determined in various ways. It is also important to determine proper initial positions of bubbles to obtain a high quality of mesh efficiently for the three-dimensional domains. Yokoyama *et al.* (1999) proposed the same mapping method as used in two dimensions. In the present work, we use the modified octree technique (Yerry and Shephard 1984) to discretize three-dimensional bodies. The modified octrees in the three-dimensional domains are illustrated in Fig. 3. The initial bubbles are then placed at the vertices of the modified octrees. Our experience has shown that the present method gives rise to better shapes of initial mesh than the method proposed by Yokoyama *et al.* (1999) even though calculation time increases.

2.2 System of dynamic bubbles

The bubbles are moved dynamically by using a physical model. The centers and radii of bubbles

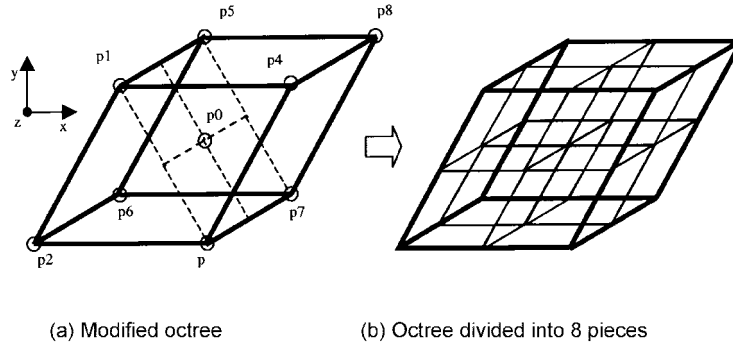


Fig. 3 A modified octree technique

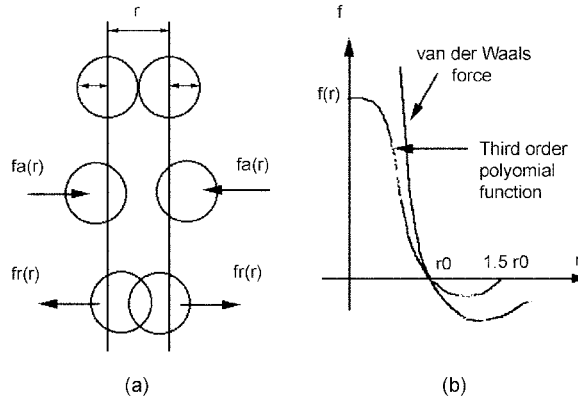


Fig. 4 Interbubble proximity-based forces : (a) target stable distance, (b) the simplified approximate force and the exact van der Waals force

determine the motions of the bubbles in a domain, wherein the bubbles ultimately reach their stabilized equilibrium position. The following system of equation of motion is considered in the bubble packing method:

$$m_i \frac{d^2 \mathbf{a}_i}{dt^2} + c \frac{d\mathbf{a}_i}{dt} = \mathbf{f}_i \quad (i = 1, 2, \dots, M) \quad (1)$$

where m_i are the masses of the bubbles, c the coefficient of viscosity, \mathbf{a}_i the position vectors of the bubble centers, M the total number of bubbles and \mathbf{f}_i the resultant force acting on i -th bubble. The system of Eq. (1) describes the process of physical relaxation, which eventually moves the bubbles to proper equilibrium positions. The force \mathbf{f}_i , which depends on the position \mathbf{x}_i and the distances from its center to the centers of the neighboring bubbles, is modeled by the van der Waals force. Let r denote the distance between the centers of two adjacent bubbles. Then, van der Waals reactions on the bubbles are approximated by the 3rd order polynomials (Shimada *et al.* 1997) in the present study, as shown in Fig. 4:

$$f(r) = \begin{cases} ar^3 + br^2 + cr + d, & 0 \leq r \leq 1.5r_0 \\ 0, & r < 0, 1.5r_0 < r \end{cases} \quad (2a)$$

$$f(r_0) = 0, f(1.5r_0) = 0, f'(0) = 0, f'(r_0) = -k_0 \quad (2b)$$

where $f(r)$ indicates the magnitude of the force between the two neighboring bubbles, and k_0 is the linear elastic constant at the equilibrium distance r_0 . Note that the force at $r = 0$ is not infinite in this model, and the forces are activated within a limited distance ($r < 1.5r_0$). The finite force at $r = 0$ prevents a singular case when the centers of bubbles coincide with each other. To reduce the calculation time, only the bubbles in a limited distance ($r < 1.5r_0$) are considered in the present bubble packing method.

The initial forces $f_i(r)$ are defined from the initial bubbles, and the final positions should be determined by enforcing the system of Eq. (1) via iteration until equilibrium state is reached, i.e.,

$$f_i = \mathbf{0} \quad (i = 1, 2, \dots, M) \quad (3)$$

We employ the 4th order Runge-Kutta method to solve the system of Eq. (1).

2.3 Control of the number of bubbles

To obtain a high quality of mesh, it is necessary to add or delete bubbles in the course of solving the equation of motion for the dynamic system presented in the previous section. If the control of the number of bubbles is not carried out, a poor mesh may be obtained as a result of inadequate number of bubbles. Shimada *et al.* (1997) suggested that a bubble surrounded with six neighboring ones leads to an optimal mesh in the two-dimensional domains while twelve adjoining bubbles around each one yield an optimal mesh in the three-dimensional domains. Consequently, more than 6 bubbles in two dimensions should be deleted, and less than 6 bubbles require addition of bubbles in the domains with a uniform mesh density. Similarly, three-dimensional bubbles can be added and deleted by the similar procedure. However, these optimal values fail to result in optimal meshes for domains with nonuniform mesh density. For an optimal mesh, nonuniform mesh density requires flexible variation in the numbers of the neighboring bubbles. In the present study, five to eight bubbles are chosen in the two-dimensional domains, and ten to eighteen bubbles in the three-dimensional domains. Our expression reveals that the control of bubble population may be performed automatically when the system of bubbles is relatively stable. Once the domain is filled with bubbles, mesh nodes are placed at the centers of these bubbles. The procedures of the bubble packing method in two and three dimension are illustrated in Fig. 5 and Fig. 6, respectively.

In the present study, the bubble packing on three-dimensional boundary surfaces is carried out independently by using the techniques of the two-dimensional bubble packing to place the bubbles on three dimensional surfaces. Such reconstruction of the bubbles on three-dimensional surfaces provides an improved quality in three-dimensional meshes: Fig. 7(a) shows bubbles obtained from the straightforward Delaunay triangulation, which is known as Bowyer's algorithm (George 1991, Bowyer 1981), while Fig. 7(b) shows the mesh obtained from the two-dimensional bubble packing applied for the boundary surface of the three-dimensional domain. The comparison is plotted in Fig. 8, in which the number of population controls and iterations are 2 and 30, respectively. In Fig. 8, tau means the ratio of minimum to maximum edge lengths. Therefore the larger distribution for the

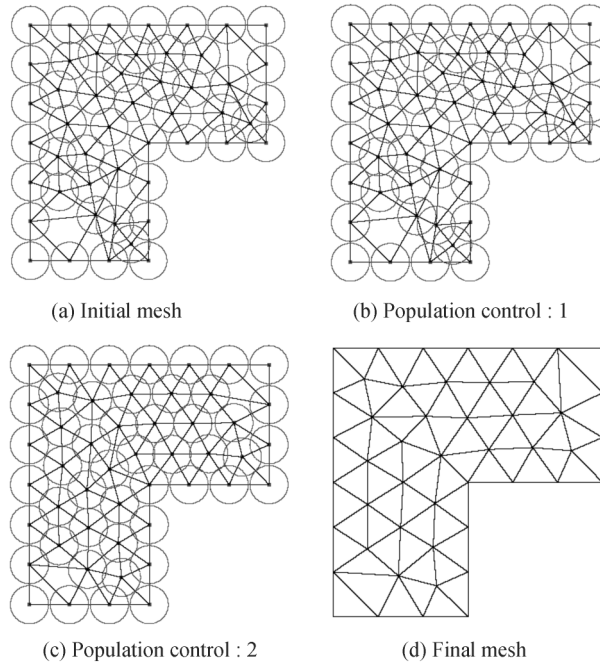


Fig. 5 Procedure of the bubble packing method for an L-shaped domain in the two-dimensional domains

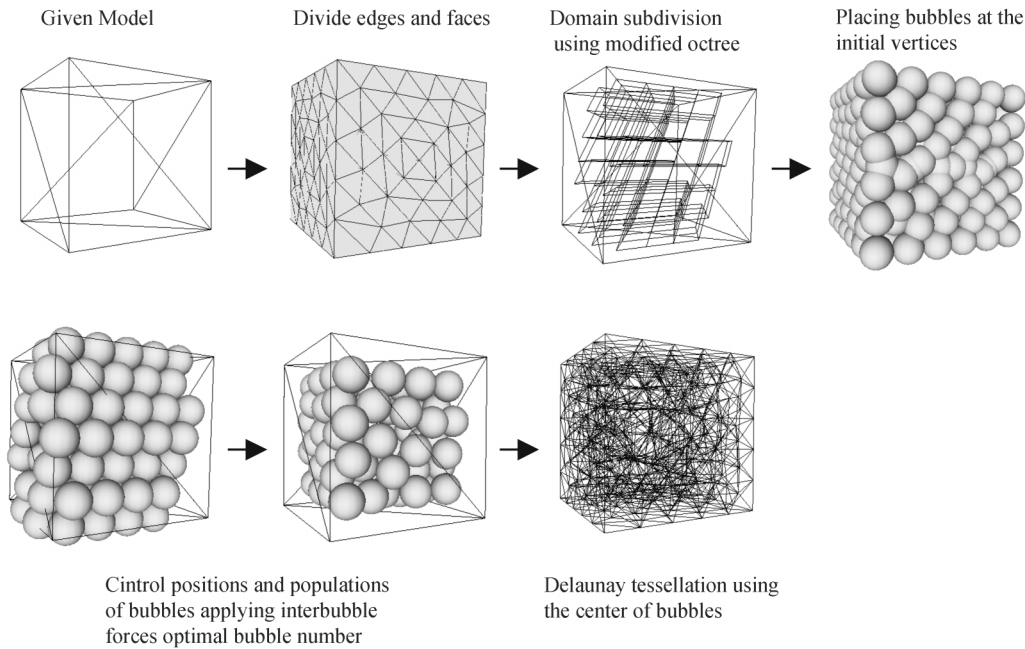


Fig. 6 Procedure of the bubble packing method for a three-dimensional cube

values of tau near tau=1 will lead to the better mesh. In Fig. 8, we see that the present method results in the larger distribution over the values of tau greater than 0.8 in comparison to Bowyer's

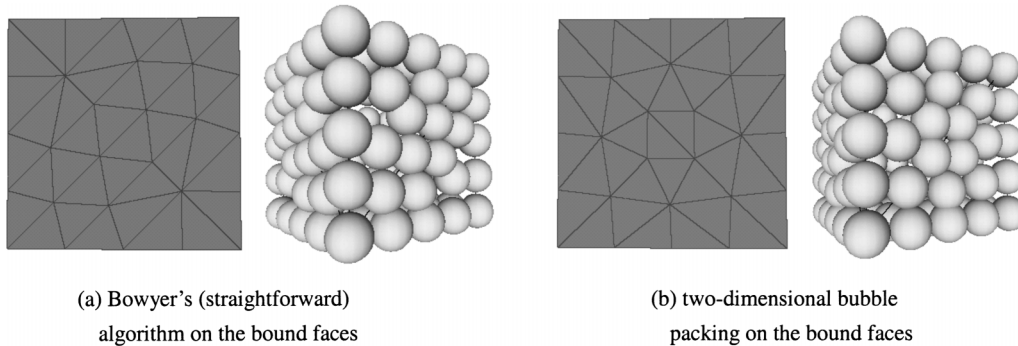


Fig. 7 Meshes obtained from Bowyer's scheme and the two-dimensional bubble packing on the bound faces of a three-dimensional model

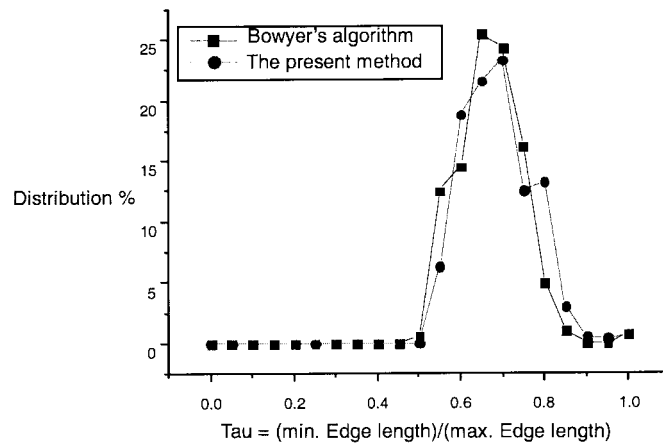


Fig. 8 Comparison of the mesh quality of two-dimensional bubble packing on bound faces of a three-dimensional model with the results obtained from the Bowyer's algorithm.

scheme, and that this indicates the improvement of the mesh quality.

3. Adaptive mesh generation

A great deal of efforts has been made to improve numerical solutions by adaptive remeshing. A proper error estimator is required for mesh design because small sized elements (*h*-adaptivity) or high order elements (*p*-adaptivity) are needed in a region with a large error. In the present study, *h*-adaptivity is mainly considered to perform adaptive mesh generation. Adaptive mesh generation has been applied to many engineering problems, but successive refinement using conforming finite elements involves time-consuming tedious work. Accordingly, an efficient method is needed to generate a mesh on the basis of a mesh density function deduced by a proper error estimator.

3.1 Error estimator

Let us consider a problem of the form (Zienkiewicz and Zhu 1991):

$$\mathbf{L}\mathbf{u} = \mathbf{S}^T\mathbf{D}\mathbf{S}\mathbf{u} = \mathbf{f} \quad \text{in } \Omega \quad (4)$$

with

$$\boldsymbol{\varepsilon} = \mathbf{S}\mathbf{u} \quad \text{and} \quad \boldsymbol{\sigma} = \mathbf{D}\mathbf{S}\mathbf{u} \quad (5)$$

where \mathbf{u} is the displacement vector, \mathbf{D} the elastic modulus tensor, $\boldsymbol{\varepsilon}$ the strain tensor, and $\boldsymbol{\sigma}$ the stress tensor. The interpolation error is defined as

$$\mathbf{e} = \mathbf{u} - \mathbf{u}^h \quad (6)$$

with

$$\mathbf{u}^h = \mathbf{N}\bar{\mathbf{u}}. \quad (7)$$

where \mathbf{N} represents the shape functions of finite elements, and $\bar{\mathbf{u}}$ the nodal displacements. The energy norm error in a domain Ω is given as:

$$\|\mathbf{e}\| = \left[\int_{\Omega} (\mathbf{S}\mathbf{e})^T \mathbf{D} (\mathbf{S}\mathbf{e}) d\Omega \right]^{1/2} = \left[\int_{\Omega} \mathbf{e}_{\sigma}^T \mathbf{D}^{-1} \mathbf{e}_{\sigma} d\Omega \right]^{1/2} \quad (8)$$

where $\mathbf{e}_{\sigma} = \mathbf{D}\mathbf{e}$. Since the exact solutions in general are not known, the error norm (8) is not evaluated directly. However, a solution \mathbf{u}^* with a higher accuracy than \mathbf{u}^h may be used instead of the exact solution \mathbf{u} in order to estimate the error in a domain. Hence the energy norm error is now approximated by

$$\begin{aligned} \|\mathbf{e}\| &\approx \|\tilde{\mathbf{e}}\| \equiv \left[\int_{\Omega} (\mathbf{S}(\mathbf{u}^* - \mathbf{u}^h))^T \mathbf{D} (\mathbf{S}(\mathbf{u}^* - \mathbf{u}^h)) d\Omega \right]^{1/2} \\ &= \left[\int_{\Omega} (\boldsymbol{\sigma}^* - \boldsymbol{\sigma}^h)^T \mathbf{D}^{-1} (\boldsymbol{\sigma}^* - \boldsymbol{\sigma}^h) d\Omega \right]^{1/2} \end{aligned} \quad (9)$$

Zienkiewicz and Zhu (1989, 1991) proposed the projection of the stresses for a better approximation. The continuous stresses is obtained by

$$\boldsymbol{\sigma}^* = \mathbf{N}\bar{\boldsymbol{\sigma}}^* \quad (10)$$

with

$$\int_{\Omega} \mathbf{P}^T (\boldsymbol{\sigma}^* - \boldsymbol{\sigma}^h) d\Omega = 0 \quad (11)$$

where \mathbf{P} is a projection operator. In general, for \mathbf{P} the shape function \mathbf{N} of finite elements is used, and this choice corresponds to the least square (L_2) continuous approximation (see Zienkiewicz and Zhu 1991).

3.2 Adaptivity and mesh density functions

The accuracy in a domain can be estimated by the relative error (Samuelsson *et al.* 1993), defined as:

$$\eta = \frac{\|e_i\|}{\|\bar{e}\|} \quad \text{with} \quad \|\bar{e}\|^2 = (\|\mathbf{u}\|^2 + \|e\|^2)/M \quad (12)$$

where $\|e_i\|$ indicates the energy norm of error associated with an element i ($i = 1, 2, \dots, M$), and M is the total number of elements. Note that $\|\bar{e}\|^2$ is the value of $\|\mathbf{u}\|^2 + \|e\|^2$ averaged by M and it assumes the average value per element. In general, the mesh should satisfy the requirement that η is less than a specific value $\bar{\eta}$. The mesh should be generated such that the following inequality may hold:

$$\eta \leq \bar{\eta} \quad (13)$$

As a result, the permissible error for an element i is written as:

$$\|e_i\| < \bar{\eta} \|\bar{e}\| \equiv \bar{e} \quad (14)$$

An optimal mesh may be obtained if the error in energy norm is equal in each element. The elements which do not satisfy the above inequality (14) are subjected to refinement. The refinement index is defined as

$$\xi_i = \frac{\|e_i\|}{\bar{e}} \quad (15)$$

Consequently, the elements with $\xi_i > 1$ may be refined. Zienkiewicz and Zhu (1991) proposed a method to predict the mesh size. The new mesh sizes are determined by

$$h_{new}^i = h_{existing}^i / \xi_i^{1/p} \quad (16)$$

where p is the order of elements, and h_{new}^i and $h_{existing}^i$ the new and the existing mesh sizes of an element “ i ”. The estimated mesh sizes in general show very good performance in the linear elasticity problems. Once mesh density functions are defined in all parts of the domain, a new mesh can be generated by the bubble packing method and the Delaunay triangulation.

4. Numerical experiments

We are concerned with only h -adaptivity in numerical experiments. The Zienkiewicz and Zhu (Z^2) error estimator is used to estimate mesh density functions, and the bubble packing method proposed here is applied to a square block and an L-shaped region in two and three dimensions. Results by Fuchs (1997) and Boender (1994) are compared with the results from the present method. The damping ratio ($c/2\sqrt{mk}$) in the system of Eq. (1) is taken to be 0.7 in all examples.

4.1 A two-dimensional square block

A square block in two dimensions is considered, as shown in Fig. 9. The uniform traction is applied on the left side, and the fixed boundary condition is applied on the bottom side, as shown in Fig. 9. The Young's modulus and Poisson's ratio are 1.0 and 0.3, respectively. The height and width of the model are both 1.0, and the plane strain condition is applied in this example. The allowable error is $\bar{\eta} = 5.0\%$, and Bowyer's algorithm (George 1991) for the Delaunay triangulation is utilized to construct a mesh. The mesh is adaptively generated by the bubble packing method and

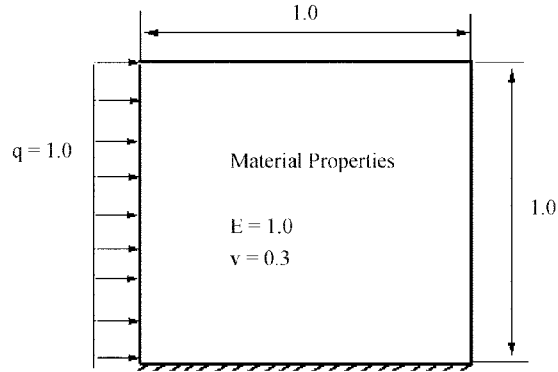


Fig. 9 A square block

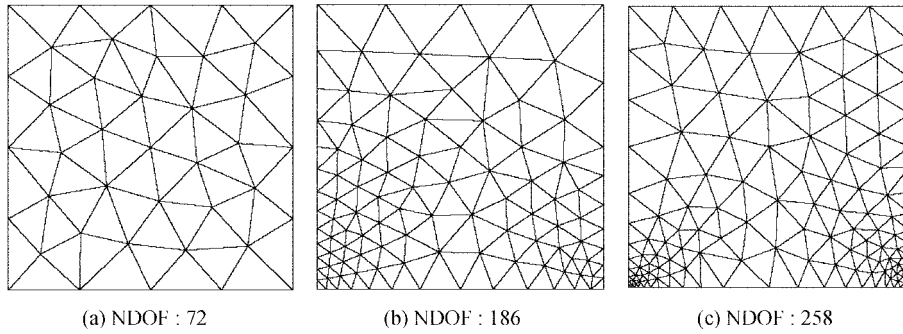


Fig. 10 Meshes obtained from the bubble packing method for the square block

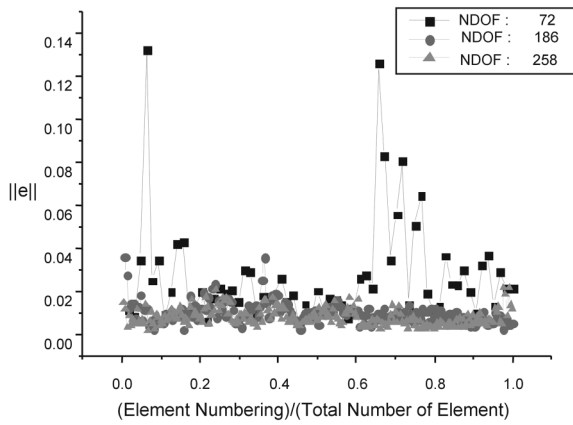


Fig. 11 Distribution of errors in elements in each refinement process for the square block

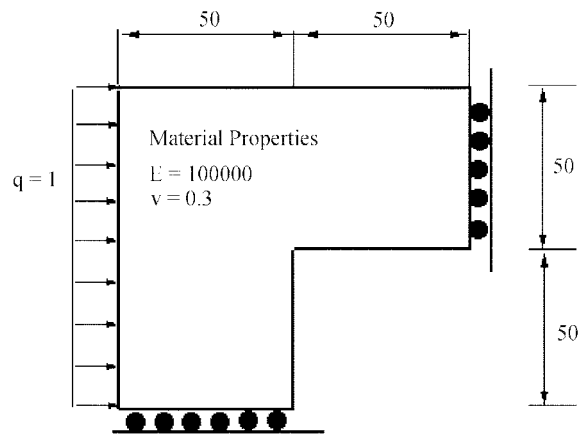


Fig. 12 An L-shaped domain in plain stress condition

the Delaunay triangulation. Fig. 10 shows the adaptive mesh generations for this example. The errors in elements in the bubble packing method are plotted in Fig. 11, in which a noticeable decrease of errors is observed as the number of elements increases.

4.2 A two-dimensional L-shaped region

Next, we consider a two-dimensional L-shaped region, as shown in Fig. 12. The uniform traction is applied on the left side, and the roller boundary conditions are applied on the end edges of the L-shaped region, as shown in Fig. 12. The Young's modulus and Poisson's ratio are 1.0×10^5 and 0.3, respectively. Plane stress condition is considered in this example. The allowable error is $\bar{\eta} = 5.0\%$, and Bowyer's algorithm (George 1991, Bowyer 1981) is employed to construct an initial mesh. By using the Z^2 error estimator and the bubble packing method, mesh is refined as shown in Fig. 13. Note that meshes obtained by the bubble packing method consist of triangular elements with regular shapes. Samuelsson *et al.* (1993) employed the advancing front technique to distribute nodes according to the density function prescribed on the domain. Comparison with the results by Samuelsson *et al.* (1993) is presented in Fig. 14. In this figure, we see that the present bubble packing method leads to a better quality of mesh than the Samuelsson's advancing front method. The errors in this example drastically diminish as the mesh is refined, as shown in Fig. 15.

4.3 A three-dimensional cube

The square block in the two-dimensional domain is extended to a three-dimensional cube. The cube dimension is $40 \times 40 \times 40$ (see Fig. 16), and the same material properties as for the preceding two-dimensional L-shaped region are employed here. The loading and the boundary conditions are as given in Fig. 9: the thickness dimension is now 40 instead of the plane strain condition of Fig. 9. The allowable error is $\bar{\eta} = 0.5\%$ in this three-dimensional example. The nodes on the surfaces are controlled independently by the bubble packing method in two dimensions. The modified octree technique is used to place initial bubbles, and the straightforward Delaunay tessellation is employed to generate a three-dimensional mesh. The bubble packing method is then applied and obtained is a mesh as in Fig. 16. Then one adaptive mesh refinement is conducted in conjunction with the bubble packing. This leads to a substantial reduction of the errors as indicated in Fig. 17.

4.4 Three dimensional L-shaped region

Next, the L-shape model shown in Fig. 12 is extended to a three-dimensional model by increasing

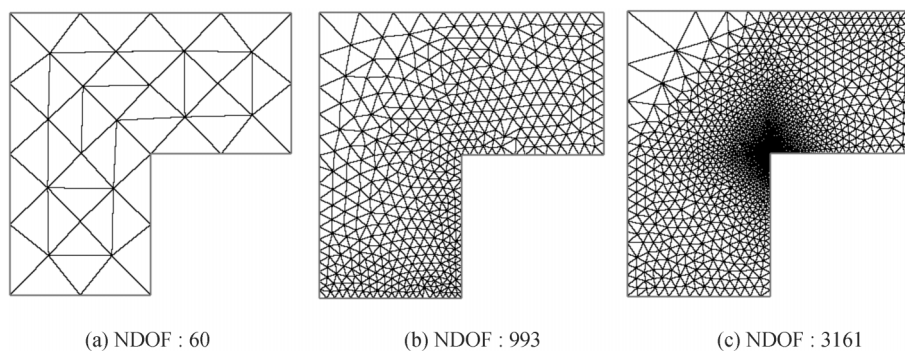


Fig. 13 Meshes obtained from the bubble packing method for the L-shaped domain

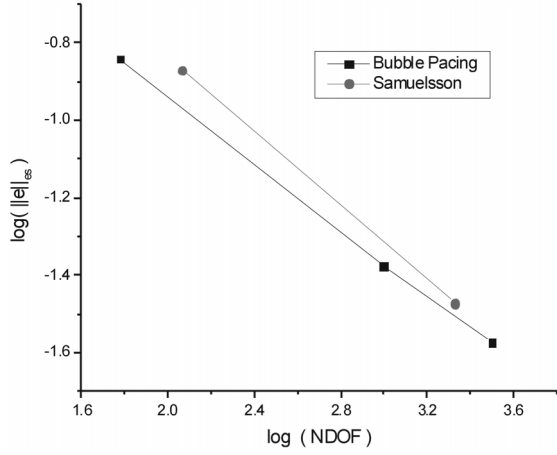


Fig. 14 Comparison with Samuelsson's results for the L-shaped domain

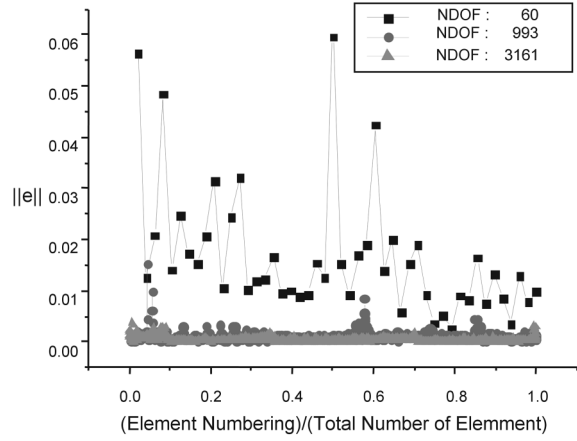


Fig. 15 Distribution of errors in elements in each remeshing process for the L-shaped domain

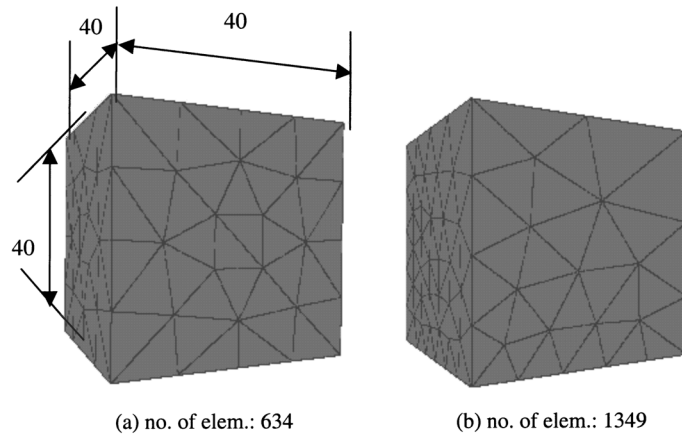


Fig. 16 Meshes obtained from the bubble packing method for the three-dimensional cube

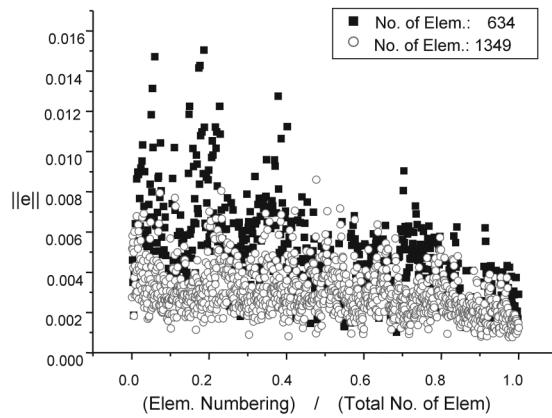


Fig. 17 Distribution of errors in elements in each remeshing process for the three-dimensional cube

the thickness. The dimension of the three-dimensional L-shaped block is shown in Fig. 18, and the same material properties as for the preceding two-dimensional L-shaped region are employed. The loading and the boundary conditions of Fig. 12 are imposed here except that the thickness dimension is now 40 instead of the plane stress condition of Fig. 12. The nodes on the surfaces are controlled independently of the interior nodes by the bubble packing method as used in the two-dimensional domains. The modified octree technique is utilized to place initial bubbles. Fig. 18 shows the meshes obtained by the present bubble packing method. The tetrahedrons constructed in this example turn out to be close to regular shapes, which is an important advantage of the bubble packing method. Fig. 19 shows that the adaptive remeshing, based on the present bubble packing scheme, reduces the overall errors noticeably.

Before closing, the time for iteration to reach equilibrium of the bubbles may be an issue for

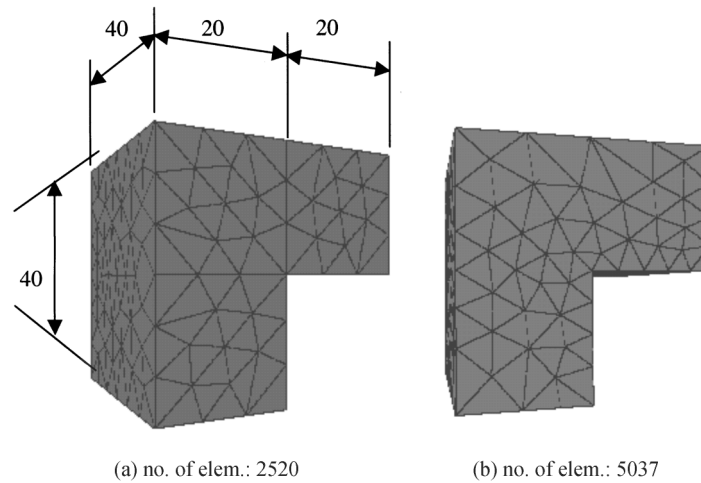


Fig. 18 Meshes obtained from the bubble packing method for the three-dimensional L-shaped block

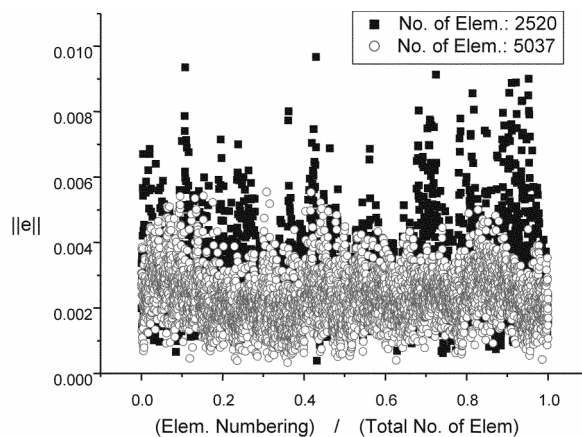


Fig. 19 Distribution of errors in elements in each remeshing process for the three-dimensional L-shaped block

linear problems. Typically in the last example of the L-shaped three-dimensional domain, the time for equilibrium of bubbles is several times greater than the solution time. Actually it largely depends on the details of coding, and so could be further reduced if the coding is implemented in an efficient manner. In nonlinear problems involving large deformations, on the other hand, the solution time greatly increases due to many time steps and iterations for equilibrium correction, and the time required for bubble packing usually is much smaller than the solution time. This is why we have not paid that much attention to the time required for bubble packing.

5. Conclusions

The bubble packing method in two and three dimensions is developed. Bubbles on three-dimensional boundary surfaces are controlled independently of the interior bubbles of the domains in order to obtain an improved quality of mesh in three-dimensional problems. The modified octree technique is employed to place initial bubbles. Meshes of high quality were obtained, and leading to a drastic reduction of errors for each of the two- and three-dimensional domains, from the present bubble packing technique combined with the adaptive refinement based upon Zienkiewicz and Zhu error estimator. Furthermore, the mesh density is straightforwardly controllable in the present procedure. Numerical examples show that the bubble packing method may be a useful tool for automatic mesh generation in two and three dimensions.

Acknowledgments

The authors would like to thank the Ministry of Science and Technology, Korea, for the financial support by a grant from the Critical Technology 21 Project.

References

- Boender, E. (1994), "Reliable Delaunay-based mesh generation and mesh improvement", *Comm. Numer. Methods Eng.*, **10**, 773-783.
- Borouchaki, H. and Lo, S.H. (1995), "Fast Delaunay triangulation in three dimensions", *Comp. Methods Appl. Mech. Eng.*, **128**, 153-167.
- Borouchaki, H. and George, P.L. (1996), "Optimal Delaunay point insertion", *Int. J. Numer. Methods Eng.*, **39**, 3407-3437.
- Bowyer, A. (1981), "Computing Dirichlet tessellations", *The Computer Journal*, **24**, 162-165.
- Choi, C.K., Lee, G.H. and Chung, H.J. (2002), "An adaptive analysis in the element-free Galerkin method using bubble meshing technique", *Comp. Struct. Eng. Inst. Korea*, **15**, 84-95.
- Cingoski, V., Murakawa, R., Kaneda, K. and Yamashita, H. (1997), "Automatic mesh generation in finite element analysis using dynamic bubble system", *J. Appl. Phys.*, **81**, 4085-4087.
- Dwyer, J.O. and Evans, P. (1997), "Triangular element refinement in automatic mesh generation", *IEEE Transactions on Magnetics*, **33**, 1740-1743.
- Frey, P.J., Borouchaki, H. and George, P.L. (1998), "Delaunay tetrahedralization using an advancing front approach", *Comp. Methods Appl. Mech. Eng.*, **157**, 115-132.
- Fuchs, A. (1997), "Almost regular Delaunay-triangulations", *Int. J. Numer. Methods Eng.*, **40**, 4595-4610.
- George, P.L. (1991), *Automatic Mesh Generation*, J. Wiley, New York.

- Lee, G.H., Choi, C.K. and Chung, H.J.(2000), "An adaptive analysis in the element-free Galerkin method using bubble meshing technique", *European Congress on Computational Methods in Applied Sciences and Engineering*, Barcelona, Spain.
- Lo, S.H. (1989), "Delaunay triangulation of non-convex planar domains", *Int. J. Numer. Methods Eng.*, **28**, 2695-2707.
- Lohner, R. (1996), "Progress in grid generation via the advancing front technique", *Eng. Comp.*, **12**, 186-210.
- Miller, G.L., Talmor, D., Teng, S.H., Walkington, N. and Wang, H. (1998), "Control volume meshes using sphere packing generation, refinement and coarsening", *Lecture Notes in Computer Science*, **1457**, 128-131.
- Rivara, M.C. (1997), "New longest-edge algorithm for the refinement of unstructured triangulations", *Int. J. Numer. Meth. Eng.*, **40**, 3313-3324.
- Samuelsson, A., Wiberg, N.E. and Zeng, L.F. (1993), "The effectivity of the Zienkiewicz Zhu error estimate and two 2D adaptive mesh generators", *Comm. Numer. Meth. Eng.*, **9**, 687-699.
- Shimada, K., Yamada, A. and Itoh, T. (1997), "Anisotropic triangular meshing of parametric surfaces via close packing of ellipsoidal bubbles", *Proc. 6th Int. Meshing Roundtable*, Sandia National Laboratories, 375-390.
- Watson, D.F. (1981), "Computing the n-dimensional Delaunay Tessellations with applications to Voronoi polytopes," *The Computer Journal*, **24**, 167-172.
- Weatherill, N.P. (1994), "Efficient three-dimensional Delaunay triangulation with automatic point creation and imposed boundary constraints", *Int. J. Numer. Methods Eng.*, **37**, 2005-2039.
- Yamakawa, S. and Shimada, K. (2000), "High quality anisotropic tetrahedral mesh generation via ellipsoidal bubble packing", *Proc. 9th International Meshing Roundtable*, New Orleans, 263-273.
- Yerry, M.A. and Shephard, M.S. (1984), "Three-dimensional mesh generation by modified octree technique", *Int. J. Numer. Meth. Eng.*, **20**, 1965-1990.
- Yokoyama, T., Cingoski, V., Kaneda, K. and Yamashita, H. (1999), "3-D automatic mesh generation for FEA using dynamic bubble system", *IEEE Transaction on Magnetics*, **35**, 1318-1321.
- Zienkiewicz, O.C. and Zhu, J.Z. (1989), "Error estimates and adaptive refinement for plate bending problems", *Int. J. Numer. Meth. Eng.*, **28**, 2839-2853.
- Zienkiewicz, O.C. and Zhu, J.Z. (1991), "Adaptivity and mesh generation", *Int. J. Numer. Meth. Eng.*, **32**, 783-810.